Int. J. Multiphase Flow, Vol. 3, pp. 61–66. Pergamon/Elsevier, 1976. Printed in Great Britain.

LAMINAR BOUNDARY LAYERS AT A MOVING INTERFACE GENERATED BY COUNTER-CURRENT GAS–LIQUID STRATIFIED FLOW

CHR. BOYADJIEV, PL. MITEV and V. BESHKOV

Central Laboratory for Chemical Engineering, Bulgarian Academy of Sciences, Geo Milev, bl. 5, Sofia 13, Bulgaria

(*Received* 21 *July* 1975)

Abstract—An experimental and theoretical investigation of the velocity distribution in the laminar boundary layers at a moving interface generated by a counter-current gas–liquid stratified flow has been made. No similarity solution of the problem exists, as in the case of co-current motion of the phases. The solution is carried out by means of the perturbation method. A comparison of the theoretical results with experimental ones obtained by the use of hot-wire technique is performed.

In several papers, see *e.g.* Boyadjiev *et al.* Part I (1976), it is shown that there is a similarity solution of the laminar boundary layers equations at the moving interface between co-current streams. In the case of counter-current flow, due to the continuity of the stress tensor at the interface no similarity solution of the problem exists and it is impossible to solve the problem in terms of a simple parameter $\theta_1 = -U_L^\infty / U_G^\infty$.

Let us consider a counter-current gas–liquid stratified flow, figure 1. In the approximations of the boundary layer theory we can write the equations of motion and continuity as follows:

$$U_G \frac{\partial U_G}{\partial X_G} + V_G \frac{\partial U_G}{\partial Y_G} = \frac{\partial^2 U_G}{\partial Y_G^2}, \qquad [1]$$

$$\frac{\partial U_G}{\partial X_G} + \frac{\partial V_G}{\partial Y_G} = 0,$$

$$U_L \frac{\partial U_L}{\partial X_L} + V_L \frac{\partial U_L}{\partial Y_L} = \frac{\partial^2 U_L}{\partial Y_L^2},$$

$$\frac{\partial U_L}{\partial X_L} + \frac{\partial V_L}{\partial Y_L} = 0,$$

$$X_G = 0, \quad Y_G \geq 0, \quad U_G = 1,$$

$$X_G \geq 0, \quad Y_G \to \infty, \quad U_G = 1,$$

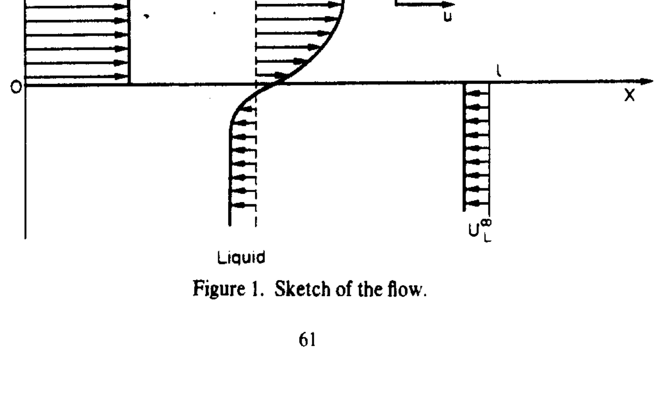

Figure 1. Sketch of the flow.

$$X_G > 0,\quad Y_G = 0,\quad U_G = -\theta_1 U_L/_{Y_L=0},\quad V_G = 0,$$
$$X_L = 0,\quad Y_L \geq 0,\quad U_L = 1,$$
$$X_L \geq 0,\quad Y_L \to \infty,\quad U_L = 1,$$
$$X_L > 0,\quad Y_L = 0,\quad \frac{\partial U_L}{\partial Y_L} = \theta_2 \frac{\partial U_G}{\partial Y_G}\bigg|_{Y_G=0}\quad Y_L = 0.$$

Here

$$X_G = x/l,\ Y_G = y/l \cdot Re^{-1/2},\ U_G = u_G/U_G^{\infty},\ V_G = v_G/U_G^{\infty} \cdot Re_G^{-1/2}$$
$$X_L = (l-x)/l,\ Y_L = -y/l \cdot Re_L^{-1/2},\ U_L = -u_L/U_L^{\infty},\ V_L = -v_L/U_L^{\infty} \cdot Re_L^{-1/2},$$
$$U_L^{\infty} > 0,\ Re_G = U_G^{\infty} \cdot l/\nu_G,\ Re_L = U_L^{\infty} \cdot l/\nu_L,$$
$$\theta_1 = (U_L^{\infty}/U_G^{\infty}) > 0,\ \theta_2 = (\mu_G/\mu_L)(\nu_L/\nu_G)^{1/2}(U_G^{\infty}/U_L^{\infty})^{3/2}. \qquad [2]$$

The solution of [1] for the gas–liquid flow can be obtained as a series expansion of the powers of the small parameters θ_1 and θ_2 (Boyadjiev *et al.* 1976):

$$U = U^{(0)} + \theta_1 U^{(1)} + \theta_2 U^{(2)} + \theta_1^2 U^{(11)} + \theta_2^2 U^{(22)} + \theta_1\theta_2 U^{(12)} + \cdots. \qquad [3]$$

If one substitutes this series for U_G, V_G, U_L and V_L in [1], the different equations for each term can be derived.

For the zeroth approximation for the gas and liquid velocity components one finds the known solutions (Boyadjiev 1971, Boyadjiev & Piperova 1971):

$$U_G^{(0)} = f'(\eta),\quad \eta = Y_G/\sqrt{(X_G)},\quad U_L^{(0)} \equiv 1, \qquad [4]$$

i.e. no gas–liquid interaction exists.

In the consequent approximations for the gas velocity terms related with θ_1 one achieves the solution (Boyadjiev 1971, Boyadjiev & Piperova 1971):

$$U_G^{(1)} = -(1/\alpha)f''(\eta),\quad U_G^{(11)} = F'(\eta). \qquad [5]$$

Here, $U_G^{(1)}$ accounts the effect of $U_L^{(0)}$ on the gas flow and $U_G^{(11)}$, the nonlinear effects of superposition of the flows $U_G^{(0)}$ and $U_G^{(1)}$. The functions f and F are found as a solution of

$$2f''' + ff'' = 0,$$
$$2F''' + fF'' + f''F = -(1/\alpha^2)f'f''' \qquad (\alpha = f''(0)),$$
$$\eta = 0,\ f = f' = F = F' = 0;\quad \eta \to \infty,\ f' = 1,\ F' = 0.$$

All other linear approximations for the powers of θ_1 and θ_2 are equal to zero, except $U_L^{(2)}$, which is obtained as a solution of

$$\frac{\partial U_L^{(2)}}{\partial X_L} = \frac{\partial^2 U_L^{(2)}}{\partial Y_L^2}, \qquad [6]$$

$$X_L = 0,\ Y_L \geq 0,\ U_L^{(2)} = 0,$$
$$X_L \geq 0,\ Y_L \to \infty,\ U_L^{(2)} = 0,$$
$$X_L > 0,\ Y_L = 0,\ \frac{\partial U_L^{(2)}}{\partial Y_L} = \frac{\alpha}{\sqrt{(1-X_L)}}.$$

There is no similarity solution of [6] because of the last boundary condition, but it can be easily solved by means of a Laplace transform:

$$\bar{u} = \int_0^\infty e^{-sX_G} U_L^{(2)}(X_G, Y_G)\, dX_G. \qquad [7]$$

For $U_L^{(2)}$ we can write:

$$U_L^{(2)} = -\frac{\alpha}{\sqrt{(\pi)}} \int_0^{X_L} \frac{\exp[-Y_L^2/4(X_L - \xi)]}{\sqrt{[(X_K - \xi)(1 - \xi)]}}\, d\xi. \qquad [8]$$

In the same way one can evaluate the other approximations, but there appear great computational difficulties. For example, the equation for $U_G^{(12)}$ is:

$$U_G^{(0)} \frac{\partial U_G^{(12)}}{\partial X_G} + U_G^{(12)} \frac{\partial U_G^{(0)}}{\partial X_G} + V_G^{(0)} \frac{\partial U_G^{(12)}}{\partial Y_G} + V_G^{(12)} \frac{\partial U_G^{(0)}}{\partial Y_G} = \frac{\partial^2 U_G^{(12)}}{\partial Y_G^2}, \qquad [9]$$

$$X_G = 0,\ U_G^{(12)} = 0,$$

$$Y_G \to \infty,\ U_G^{(12)} = 0,$$

$$Y_G = 0,\ U_G^{(12)} = \frac{\alpha}{\sqrt{(\pi)}} \int_0^{1-X_G} \frac{d\xi}{(1 - X_G - \xi)(1 - \xi)}.$$

In this case there is no similarity solution either, because of the last boundary condition.

From [3–8] one derives the velocity distribution in the laminar boundary layers at a moving interface generated by counter-current gas–liquid stratified flow:

$$U_G = f' - \frac{\theta_1}{\alpha} f'' + \theta_1^2 F',$$

$$V_G = \frac{Y_G}{2X_G} f' - \frac{1}{2\sqrt{(X_G)}} f - \frac{\theta_1}{\alpha}\left(\frac{Y_G}{2X_G} f'' - \frac{1}{2\sqrt{(X_G)}} f'\right) + \theta_1^2 \left(\frac{Y_G}{2X_G} F' - \frac{1}{2\sqrt{(X_G)}} F\right), \qquad [10]$$

$$U_L = 1 - \theta_2 \frac{\alpha}{\sqrt{(\pi)}} \int_0^{X_L} \frac{\exp[-Y_L^2/4(X_L - \xi)]}{\sqrt{[(X_L - \xi)(1 - \xi)]}}\, d\xi,$$

$$V_L = \frac{\theta_2 \alpha Y_L}{2\sqrt{(\pi)}} \int_0^{X_L} \frac{\exp[-Y_L^2/4(X_L - \xi)]}{(X_L - \xi)^{3/2}\sqrt{(1 - \xi)}}\, d\xi.$$

In figures 2–6 are shown the velocity profiles predicted by [10] (the solid lines). The equations for V_G and V_L are easily derived from the continuity equations in [1].

Equations [10] allow the determination of the laminar layer thickness in both phases

$$\delta_G = \eta_G l \sqrt{\left(\frac{X_G}{Re_G}\right)}, \quad \delta_L = \eta_L l \sqrt{\left(\frac{X_L}{Re_L}\right)} \qquad [11]$$

using the conditions

$$u_G(x, \delta_G) = 0.99 U_G^\infty, \quad u_L(x_L - \delta_L) = -0.99 U_L^\infty. \qquad [12]$$

Here η_G and η_L depend on θ_1, θ_2, x and l. In the approximations of [10], $\eta_G = \eta_G(\theta_1)$ and $\eta_L = \eta_L(\theta_2, X_L)$. For example, from figure 2 η_G and η_L can be derived: $\theta_1 = 0.05$, $\eta_G = 5.2$, $\theta_2 = 0.42$, $X_L = 0.083$, $\eta_L = 1.48$.

There is no theoretical proof for the use of the perturbation method of solution of [1] *e.g.* by comparison of [10] with the results of the exact solution, as was made in the case of co-current flow, Boyadjiev *et al.* Part I (1976). This is due to the nonsimilarity of [1]. That is why it must be

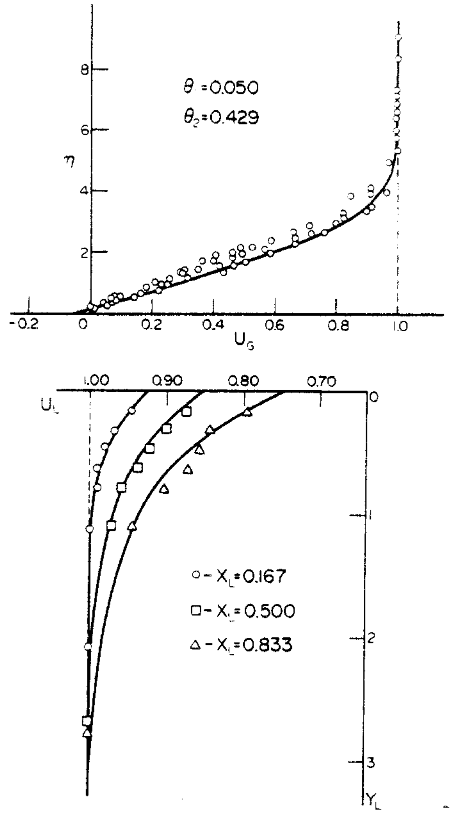

Figure 2. Theoretical (solid lines) and experimental (points) velocity profiles for $\theta_1 = 0.050$ and $\theta_2 = 0.429$.

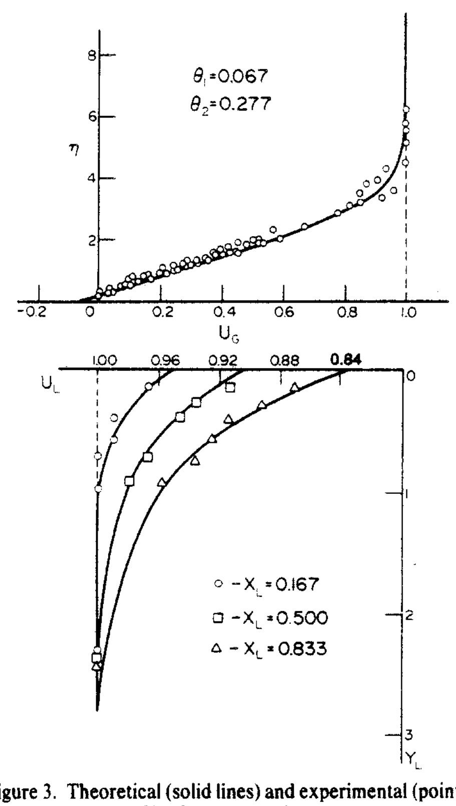

Figure 3. Theoretical (solid lines) and experimental (points) velocity profiles for $\theta_1 = 0.067$ and $\theta_2 = 0277$.

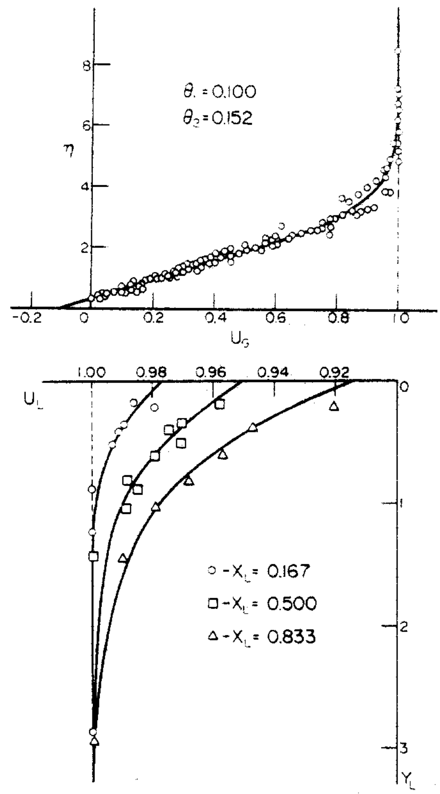

Figure 4. Theoretical (solid lines) and experimental (points) velocity profiles for $\theta_1 = 0.100$ and $\theta_2 = 0.152$.

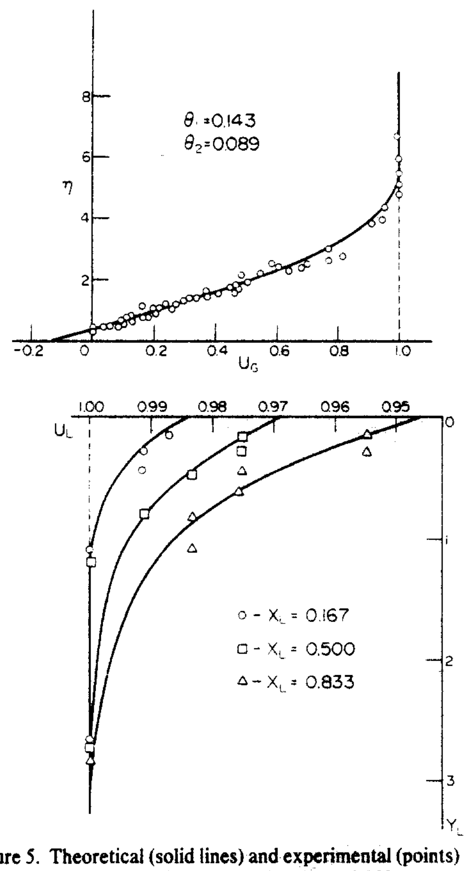

Figure 5. Theoretical (solid lines) and experimental (points) velocity profiles for $\theta_1 = 0.143$ and $\theta_2 = 0.089$.

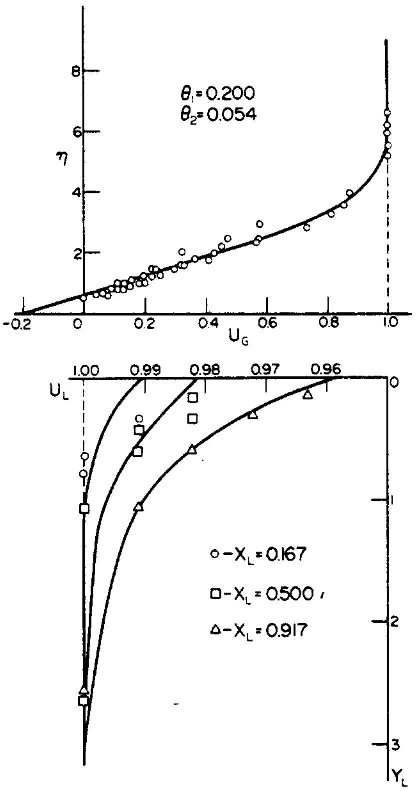

Figure 6. Theoretical (solid lines) and experimental (points) velocity profiles for $\theta_1 = 0.200$ and $\theta_2 = 0.054$.

solved numerically. The only proof for the validity of [10] for the velocity distribution in the laminar boundary layers at a moving interface by counter-current gas–liquid stratified flow can be achieved experimentally.

The experimental check of the theoretical results [10] was carried out on the laboratory apparatus described in Boyadjiev *et al.* Part 2(1976), where the counter-current flow was produced. The length of the gas–liquid interaction zone was 1.2 m and the depth 0.07 m for the liquid phase and 0.14 m for the gas phase. All experiments were carried out at a temperature 27 ± 1°C using a hot wire apparatus (DISA-type 55A01). A hot film gas probe (type 55A80) and a probe type 55A81 for the liquid phase were used. The velocities were measured for $y = \pm 1.5$ mm; ±3.0 mm; ±4.5 mm etc. until constant velocities for the potential flows in the gas and in the liquid phases were attained. The velocity profiles were measured for 12 values of x in the interval $0.1 \leq x \leq 1.2$ m, and for 5 values of $\theta_1(U_L^\infty$ varied in the interval 1.0–2.4 cm/s and U_G^∞, 7–30 cm/s). From the values obtained for $u_G(x, y)$ and $u_L(x, y)$, $U_G(\eta)$ and $U_L(X_L, Y_L)$ were calculated. The results obtained are compared in figures 2–6 with the theoretical velocity profiles, calculated from [10]. The comparison of the theoretical (U_L^T) and the experimental (U_L^E) values for θ_1 and θ_2 as shown in these figures and for $X_L = 0.083$; 0.250; 0.333; 0.417; 0.500; 0.583; 0.677; 0.750; 0.917 is performed in figure 7. The coincidence of the theoretical and experimental results is fully satisfactory. Here, one must take into account that the solution [10] is one order of magnitude less than the similar results for the case of co-current flow.

The interfacial velocity for $0 < x < 1$ can be calculated from [10]

$$u_s = U_L^\infty\left(-1 + \frac{\theta_2 \alpha}{\sqrt{(\pi)}} \ln \frac{1 + \sqrt{X_L}}{1 - \sqrt{X_L}}\right). \qquad [13]$$

The comparison of the theoretical values of the interfacial velocity U_s with the experimental ones U_s^E is shown in figure 8.

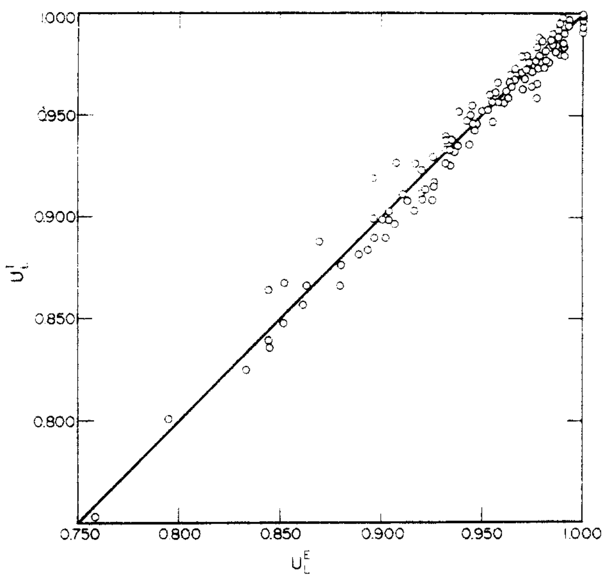

Figure 7. Comparison of the theoretical (U_L^T) and experimental (U_L^E) values of the velocity in the liquid phase for different values of θ_1, θ_2 and X_L.

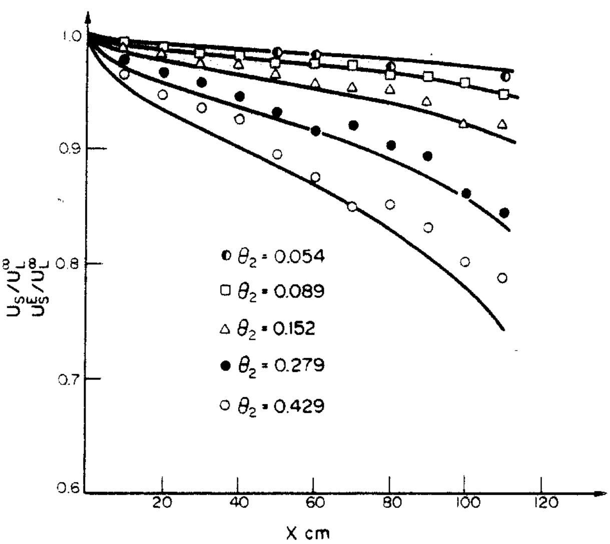

Figure 8. Comparison of the theoretical (U_s) (solid lines) and experimental (U_s^E) (points) values of the interfacial velocity.

The experimental results obtained, figures 2–8 are a proof of the validity of [10] for the evaluation of velocity profiles in laminar boundary layers at a moving interface generated by counter-current gas–liquid stratified flow.

REFERENCES

Boyadjiev, Chr., Mitev Pl. & Sapundzhiev, T. 1976 Laminar boundary layers of co-current gas–liquid stratified flows—I. Theory. *Int. J. Multiphase Flow* **3**, 51–55.

Boyadjiev, Chr. 1971 The hydrodynamics of certain two-phase flows. 1. The laminar boundary layer at a flat gas–liquid interface. *Int. Chem. Engng* **11**, 464–469.

Boyadjiev Chr. & Piperova, M. 1971 The hydrodynamics of certain two-phase flows. 4. Evaluation of some special functions. *Int. Chem. Engng* **11**, 479–487.

Mitev Pl. & Boyadjiev, Chr. 1976 Laminar boundary layers of co-current gas–liquid stratified flows—II. Velocity measurements. *Int. J. Multiphase Flow* **3**, 57–60.